

Evidence of a strongly anisotropic superconducting gap in kagome superconductor CsV_3Sb_5: A study of directional point-contact Andreev reflection spectroscopy

Yu-Qing Zhao(赵宇清), Zhi-Fan Wu(武治帆), Hai-Yan Zuo(左海艳), Wei-Ming Lao(劳威铭), Wang-Ju Yang(杨王菊), Qiu-Xia Chen(陈秋霞), Yao He(何垚), Hai Wang(王海), Wenxin Lv(吕文欣), Qi Wang(王琦), Yan-Peng Qi(齐彦鹏), Gang Mu(牟刚), Hechang Lei(雷和畅), and Cong Ren(任聪)

Citation: Chin. Phys. B, 2026, 35 (**5**): 057405. DOI: 10.1088/1674-1056/ae27b0
http://cpb.iphy.ac.cn; http://iopscience.iop.org/cpb

What follows is a list of articles you may be interested in

Exotic superconductivity in new topological kagome metal $CsTi_3Bi_5$

Jiali Liu(刘家利), Zhen Zhao(赵振), Hongqin Xiao(肖洪钦), Yuhang Zhang(张宇航), Zouyouwei Lu(鲁邹有为), Jihu Lu(卢佶虎), Feng Wu(吴凤), Chengjie Xu(徐诚杰), Hua Zhang(张华), Hui Chen(陈辉), Haitao Yang(杨海涛), Ziyi Liu(刘子儀), Xiaoli Dong(董晓莉), and Hongjun Gao(高鸿钧)

Chin. Phys. B, 2026, 35 (**2**): 027403. DOI: 10.1088/1674-1056/ae2c6d

Surface-sensitive electronic structure of kagome superconductor CsV_3Sb_5

Zhisheng Zhao(赵志生), Jianghao Yao(姚江浩), Rui Xu(徐瑞), Yuzhe Wang(王禹喆), Sen Liao(廖森), Zhengtai Liu(刘正太), Dawei Shen (沈大伟), Shengtao Cui(崔胜涛), Zhe Sun(孙喆), Yilin Wang(王义林), Donglai Feng(封东来), and Juan Jiang(姜娟)

Chin. Phys. B, 2024, 33 (**10**): 107403. DOI: 10.1088/1674-1056/ad7016

Two-fold symmetry of the in-plane resistance in kagome superconductor $Cs(V_{1-x}Ta_x)_3Sb_5$ with enhanced superconductivity

Zhen Zhao(赵振), Ruwen Wang(王汝文), Yuhang Zhang(张宇航), Ke Zhu(祝轲), Weiqi Yu(余维琪), Yechao Han(韩烨超), Jiali Liu(刘家利), Guojing Hu(胡国静), Hui Guo(郭辉), Xiao Lin(林晓), Xiaoli Dong(董晓莉), Hui Chen(陈辉), Haitao Yang(杨海涛), and Hong-Jun Gao(高鸿钧)

Chin. Phys. B, 2024, 33 (**7**): 077406. DOI: 10.1088/1674-1056/ad4ffa

Pressure tuning of the anomalous Hall effect in the kagome superconductor CsV_3Sb_5

Fang-Hang Yu(喻芳航), Xi-Kai Wen(温茜凯), Zhi-Gang Gui(桂智刚), Tao Wu(吴涛), Zhenyu Wang(王震宇), Zi-Ji Xiang(项子雾), Jianjun Ying(应剑俊), and Xianhui Chen(陈仙辉)

Chin. Phys. B, 2022, 31 (**1**): 017405. DOI: 10.1088/1674-1056/ac3990

Evolution of superconductivity and charge order in pressurized RbV_3Sb_5

Feng Du(杜锋), Shuaishuai Luo(罗帅帅), Rui Li(李蕊), Brenden R. Ortiz, Ye Chen(陈晔), Stephen D. Wilson, Yu Song(宋宇), and Huiqiu Yuan(袁辉球)

Chin. Phys. B, 2022, 31 (**1**): 017404. DOI: 10.1088/1674-1056/ac4232

Evidence of a strongly anisotropic superconducting gap in kagome superconductor CsV_3Sb_5: A study of directional point-contact Andreev reflection spectroscopy

Yu-Qing Zhao(赵宇清)[1,†], Zhi-Fan Wu(武治帆)[1,†], Hai-Yan Zuo(左海艳)[1], Wei-Ming Lao(劳威铭)[1], Wang-Ju Yang(杨王菊)[1], Qiu-Xia Chen(陈秋霞)[1], Yao He(何垚)[1], Hai Wang(王海)[1], Wenxin Lv(吕文欣)[2,3], Qi Wang(王琦)[4], Yan-Peng Qi(齐彦鹏)[4], Gang Mu(牟刚)[5], Hechang Lei(雷和畅)[2,3,‡], and Cong Ren(任聪)[1,§]

[1] *School of Physics and Astronomy, Yunnan University, Kunming* 650500, *China*
[2] *School of Physics and Beijing Key Laboratory of Opto-electronic Functional Materials and Micro-nano Devices, Renmin University of China, Beijing* 100872, *China*
[3] *Key Laboratory of Quantum State Construction and Manipulation (Ministry of Education), Renming University of China, Bijing* 100872, *China*
[4] *State Key Laboratory of Quantum Functional Materials, School of Physical Science and Technology, ShanghaiTech University, Shanghai* 201210, *China*
[5] *State Key Laboratory of Materials for Integrated Circuits, Shanghai Institute of Microsystem and Information Technology, Chinese Academy of Sciences, Shanghai* 200050, *China*

(Received 17 September 2025; revised manuscript received 1 December 2025; accepted manuscript online 4 December 2025)

In the recently discovered V-based kagome superconductors AV_3Sb_5 (A = K, Rb, Cs), superconductivity intertwines with an unconventional charge density wave (CDW), raising fundamental questions concerning the superconducting gap structure in the presence of such intertwined orders. Here, we perform the first directional point-contact Andreev reflection (PCAR) spectroscopy measurement on CsV_3Sb_5 to probe its superconducting gap structure. Strikingly distinct PCAR spectra emerge depending on the current injection direction: an in-gap zero-bias conductance peak dominates for currents parallel to the *ab*-plane, contrasting to a gap-like structure observed perpendicularly. Quantitative analysis using a modified BTK-model estimates a pronounced gap anisotropy of ∼70% with a gap minimum ∼ 0.15 meV. These results provide a foundation for further understanding the nature of the topological superconducting state on the sample edges.

Keywords: kagome superconductor, gap symmetry, Andreev reflection spectroscopy

PACS: 74.70.–b, 74.20.Rp, 74.45.+c

DOI: 10.1088/1674-1056/ae27b0 **CSTR:** 32038.14.CPB.ae27b0

1. Introduction

Kagome lattices — distinguished by their unique two-dimensional network of corner-sharing triangles — have long attracted the attention of the condensed matter physics community as fertile ground for novel quantum phenomena. These phenomena stem from the strong electron correlations and magnetic frustration inherent to the kagome geometry.[1–6] This paradigm has been significantly expanded by the recent discovery of superconductivity in vanadium-based kagome metals AV_3Sb_5 (A = K, Rb, Cs). These compounds host an ideal, non-magnetic kagome net of vanadium atoms and exhibit superconductivity with critical temperatures $T_c \sim 1$–3 K.[7–12] Intriguingly, superconductivity in these materials emerges intertwined with unconventional charge density wave (CDW) orders.[13–21] Elucidating the nature of this superconductivity and its interplay with CDW orders within the unique kagome framework, which may host mechanisms possibly distinct from that of conventional superconductivity, is now a central focus in quantum materials research.

The gap symmetry of kagome superconductors, essential for elucidating the microscopic pairing mechanism and interplay between electronic orders, has not been fully settled yet. Early experimental evidence supported a multiple isotropic s-wave gap in a strong coupling scenario.[4,22–25] However, recent studies are primarily exploring the potential for anisotropic or even nodal gaps. Thermal conductivity measurements on CsV_3Sb_5 and μSR studies on K/RbV_3Sb_5 suggest the presence of a nodal gap.[26,27] Low-temperature scanning tunneling microscopy (STM) on CsV_3Sb_5 reported both nodal and nodeless gap features co-existing over multiple Fermi surfaces.[28,29] More recently, high-resolution angle-resolved photoemission spectroscopy (ARPES) on high-quality CsV_3Sb_5 crystals revealed an anisotropy as high as $\sim$ 80% in the superconducting gap on the β-band Fermi surface,[30] suggesting a possible nodal gap structure. Intriguingly, the anisotropy observed via STM and ARPES experiments was suppressed in Ta-doped CsV_3Sb_5 with a higher T_c and without a CDW,[31–34] inducing a transition from a

[†]These authors contributed equally to this work.
[‡]Corresponding author. E-mail: hlei@ruc.edu.cn
[§]Corresponding author. E-mail: cren@ynu.edu.cn

© 2026 Chinese Physical Society and IOP Publishing Ltd. All rights, including for text and data mining, AI training, and similar technologies, are reserved.

possible nodal to a nodeless s-wave gap state. Similar suppression of gap anisotropy was observed in the magnetic penetration depth measurements on the electron-irradiated CsV_3Sb_5,[35] just like the case of the nodal $s_{\pm}$-wave superconductor $BaFe_2(As_{1-x}P_x)_2$.[36–38] This convergence of diverse, often contradictory experimental conclusions reflects the profound complexity of these materials, and the directional measurement of the superconducting gap in such a kagome superconductor is highly desired.

Directional point contact Andreev reflection spectroscopy, injecting a current through a ballistic point contact along different crystallographic directions in the superconductor, to some extent equivalent to directional tunneling spectroscopy, is a powerful tool to investigate the gap anisotropy in unconventional superconductors.[39–41] This technique allows a direct determination of the gap and its temperature dependence along various directions in the crystal. The measurement of point-contact spectroscopy can be implemented either with a metal–tip point contact[39] or soft planar contact geometry.[42] Specifically, the soft planar point contacts have the advantage of avoiding inhomogeneous pressure or local strain effects induced by the metal tip, providing a pressureless spectroscopy measurement. Another practical advantage of soft point-contact spectroscopy is that point-contact junctions can be flexibly formed on crystal surfaces with specific crystallographic orientations, enabling a systematic study of the superconducting gap symmetry associated with the crystallographic orientation.[41,42] Leveraging these capabilities, in this work we performed the first directional point contact spectroscopy measurements on large single crystals of CsV_3Sb_5 to investigate its gap symmetry. With injecting the current either along the *c*-axis or along the *ab*-plane, the central observation from these studies is the presence of an in-gap zero-bias conductance peak in *ab*-plane SPCAR spectra, in contrast to a gap-like conductance peak in *c*-axis SPCAR spectra. By comparison, we argue the presence of a strongly anisotropic gap for the *ab*-plane in CsV_3Sb_5.

2. Experiment details

Single crystals of CsV_3Sb_5 were synthesized via the self-flux method in two independent laboratories; crystals from these sources are denoted as #1 and #2, respectively. Figure 1(a) shows the temperature-dependent in-plane resistivity, $\rho_{xx}(T)$, measured on a representative CsV_3Sb_5. The crystal exhibits metallic behavior, evidenced by a residual resistivity ratio $RRR \equiv R(300\ \mathrm{K})/R(5\ \mathrm{K}) = 22$. An anomaly in $\rho_{xx}(T)$ near 92 K signifies the charge-density-wave (CDW) transition. The inset of Fig. 1(a) details the superconducting transition observed at a low temperature, revealing an onset critical temperature $T_c^{\mathrm{onset}} \simeq 3.4$ K and a zero-resistivity state below $T_c^{\mathrm{zero}} \simeq 2.8$ K.

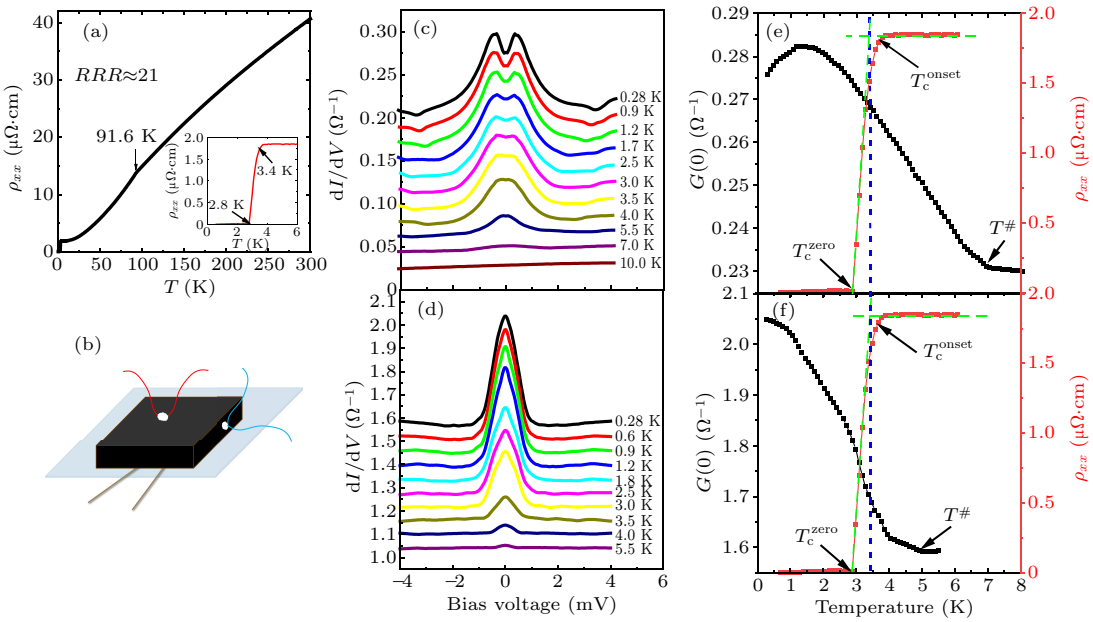


Fig. 1. (a) Temperature dependence of the in-plane resistivity ρ_{xx} of a CsV_3Sb_5 single crystal, a pronounced kink at approximately 91.6 K indicates the onset of the charge density wave (CDW) transition. The inset magnifies the low-temperature region, showing the superconducting transition with the onset temperature T_c^{onset} and zero-resistivity temperature T_c^{zero} marked. (b) Schematic of the "soft" point-contact spectroscopy measurement configuration. The black block represents the CsV_3Sb_5 single crystal, while the red and blue lines indicate the injection paths for soft point-contact Andreev reflection measurements with the current applied perpendicular (labeled as *c*-axis junction) and parallel (labeled as *ab*-plane junction) to the *ab*-plane, respectively. (c)–(d) T-dependent point-contact conductance spectra $G \equiv \mathrm{d}I/\mathrm{d}V$ measured with sensing current I along the *c*-axis (*c*-axis junction) (c) and along *ab*-plane (*ab*-plane junction), respectively. (e)–(f) T-dependence of the zero-bias conductance $G(0)$ of CsV_3Sb_5/Ag point contacts for the *c*-axis (e) and *ab*-plane junctions (f), respectively. The bulk resistivity ρ_{xx} in the superconducting transition region is presented for comparison.

Point-contact spectroscopy measurements were performed on CsV_3Sb_5 single crystals using a "soft" point-contact technique.[42] Crystals, with typical dimensions $2.5 \times 2.0 \times (0.3-0.5)$ mm^3 along the a, b, and c axes, were cleaved and/or polished to expose specific crystallographic planes. Then a droplet of silver paint bonding with Pt wires (of 16 μm in diameter) was attached to the fresh surface. The typical size of these planar contacts is about 50–80 μm under a microscope. The Ag nanoparticles of the dried silver paint create an effective hetero-contact composed of many parallel nanocontacts on the surface, analogous to a metal-tip point contact.

Two distinct junction geometries were investigated: (1) "c-axis" junctions, where metal contacts were deposited directly on the cleaved ab-plane surface; (2) "ab"-plane junctions, where metal contacts were patterned onto the surface perpendicular to the ab-plane (i.e., the ac/bc surface). To prepare the ac/bc-plane junctions, the crystal was first carefully sectioned perpendicular to the ab-plane, followed by mechanical polishing of the surface using 10000-grit silicon carbide sandpaper to achieve micro-level flatness. The resultant point-contact configurations are schematically depicted in Fig. 1(b). Differential conductance spectra, $G(V) \equiv \mathrm{d}I/\mathrm{d}V$, were measured using a standard phase-sensitive lock-in technique in a quasi-four-terminal configuration. The contact resistance R_J, dominated by the contact between the silver nanoparticles and the CsV_3Sb_5 surface, typically ranges between 0.5 Ω and 10 Ω, consistent with values expected for genuine ballistic point contacts between normal metals and superconductors.

3. Results and discussion

Figures 1(c) and 1(d) present the temperature T-dependent point-contact Andreev reflection conductance spectra, $G(V)$, measured along the c-axis and ab-plane of CsV_3Sb_5, respectively. A striking dichotomy emerges at the lowest temperature of 0.28 K: The c-axis spectrum [Fig. 1(c)] exhibits a characteristic double-peak structure at the gap edge accompanied by a zero-bias conductance dip. Conversely, the ab-plane conductance spectrum [Fig. 1(d)] displays a prominent in-gap conductance peak centered at zero bias. Qualitatively, the c-axis double-peak feature is a hallmark of nodeless superconductivity observed in intermediate-transparency junctions at finite temperatures. In contrast, the in-gap zero-bias conductance peak in intermediate-transparency junctions signifies gapless superconductivity with strongly anisotropic or even a nodal gap, reminiscent of d-wave superconductivity observed in cuprates.[43]

Another feature in these conductance spectra is that conductance spectra exhibit a significant signal at temperatures above $T_c \simeq 3.4$ K. For the c-axis junction: at $T > T_c$, the sharp coherence peaks broaden and diminish, but substantial residual Andreev conductance remains evident [Fig. 1(c)]. This excess conductance only vanishes completely at a higher characteristic temperature $T^{\#} \sim 6.5$ K. A similar phenomenon occurs for the ab-plane junction [Fig. 1(d)], where the Andreev reflection spectra persist up to $T^{\#} \sim 5.5$ K. The T-evolution of the zero-bias conductance $G(0)$, plotted alongside the in-plane resistivity ρ_{xx} in Figs. 1(e) and 11(f), provides direct evidence for this persistent conductance "tail" extending to $T^{\#}$. This robust observation of excess Andreev conductance above T_c — consistently reported in previous soft point-contact studies on KV_3Sb_5 and CsV_3Sb_5[24,25] — is reproduced across all six CsV_3Sb_5 samples measured in this study, with each exhibiting nearly identical spectroscopic behavior. The observation of excess conductance above T_c in our PCAR spectra points to intriguing physics extending beyond conventional superconductivity in CsV_3Sb_5. This phenomenon may be related to the prevailing strong electron correlations within the kagome lattice and could signal the presence of a pseudogap-like state. Unraveling the origin and implications of this anomalous conductance tail constitutes an open issue that warrants further investigation.[44]

To quantitatively determine the superconducting gap structure of CsV_3Sb_5, we performed detailed PCAR spectroscopy with the sensing current aligned parallel to both the c-axis and ab-plane junctions on two distinct samples (#1 and #2). Figures 2(a) and 2(b) present the normalized c-axis conductance spectrum $G(V)/G_N$ at the base temperature 0.28 K for junctions #1 and #2, respectively. Both junctions consistently exhibit a characteristic double-peak structure, indicative of nodeless superconductivity. Analysis using the Blonder–Tinkham–Klapwijk (BTK) model reveals that a single isotropic s-wave gap fails to reproduce the spectra. Instead, superior fits are achieved using a modified two-gap s-wave model $G(V) = \omega G^S(V) + (1-\omega)G^L(V)$, where ω quantifies the relative spectral weight of the two conductance channels. The two-gap model yields the following key parameters for the c-axis junctions: small gap Δ^S: 0.37 meV (#1), 0.45 meV (#2); large gap Δ^L: 0.78 meV (#1), 0.82 meV (#2); spectral weight $\omega \simeq 0.60$ for both samples; inelastic broadening parameter $\Gamma^S \simeq 0.13$ meV (#1), 0.15 meV (#2); junction transparency $Z \simeq 0.54$ (#1), 0.78 (#2). T-dependence of PCAR spectra confirms the model validity. Figures 2(c) and 2(d) show the PCAR spectra for samples #1 and #2, respectively, at various temperatures alongside fits using the two-gap model with the ω parameter fixed.[24,25] The broadening parameter Γ increases slightly with temperature up to T_c. The temperature dependence of Δ^L and Δ^S plotted in Figs. 2(e) and 2(f) follows the empirical BCS form $\Delta(T) = \Delta_0 \tanh(\alpha\sqrt{T_c/T-1})$ with zero-temperature gap values $\Delta_0^L \simeq 0.80$ meV and $\Delta_0^S \simeq 0.41$ meV. The extracted gap magnitudes correspond to distinct coupling strengths: Strong coupling $2\Delta_0^L/k_BT_c \simeq 5.47$, weak coupling $2\Delta_0^S/k_BT_c \simeq 2.73$. This relation $2\Delta^L/k_BT_c >$

$3.52 > 2\Delta^{S}/k_{B}T_{c}$[45] quantitatively aligns with prototypical two-gap superconductors MgB_2[42,46] and is consistent with prior reports on CsV_3Sb_5 c-axis junctions.[24,25]

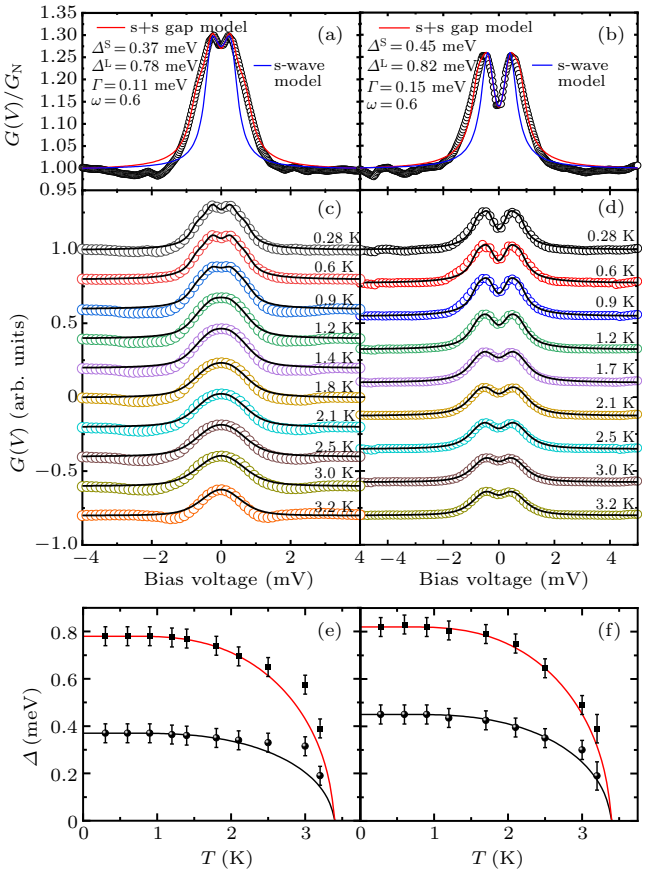


Fig. 2. (a)–(b) The normalized c-axis Andreev conductance spectrum $G(V)/G_N$ at the lowest $T = 0.28$ K for #1 and #2 junctions, respectively. The solid red curves are their BTK fits with a two-isotropic gap model. The solid blue curves are their BTK fits with a single s-wave gap model, for comparison. (c)–(d) The normalized c-axis Andreev conductance spectra $G(V)/G_N$ at various T from 0.28 K to 3.5 K for #1 (c) and #2 (d) junctions, respectively. The solid curves are their BTK fits using a two-isotropic gap model. (e)–(f) The corresponding superconducting gap Δ as a function of T, which closely follows the BCS Δ–T function.

In contrast, point-contact spectra with current $I \parallel ab$-plane [Figs. 3(a) and 3(b)] reveal a single broad zero-bias conductance peak within the gap region — a hallmark signature of anisotropic superconductivity. Guided by the six-fold symmetry of the kagome lattice and supported by ARPES measurements, we model the gap anisotropy using the functional form $\Delta^{ab}(\theta) = \Delta^{ab}[(1-r)+r\cos(6\theta)]$,[35] where θ is the azimuthal angle and r quantifies the gap anisotropy ($r = 0$ corresponds to an isotropic s-wave gap; $r = 1$ yields a fully nodal state with gap zeros). This anisotropic s-wave BTK model excellently describes the low-T normalized conductance $G(V)$. The best fits yield a gap amplitude $\Delta^{ab} \simeq 0.50$ meV for sample #1 and 0.49 meV for sample #2, with the broadening parameter $\Gamma = 0.18$ meV and anisotropy $r = 0.70 \pm 0.10$ for both junctions.

Figures 3(c) and 3(d) show the T-dependence of SPCAR spectra of ab-plane junctions together with the corresponding BTK-fitting curves. As shown, the anisotropic BTK model provides good fits to all $G(V)$ curves. In all fittings, r is kept constant for each sample, while Γ increases slightly with T up to T_c. The resulting gaps Δ for #1 and #2 are plotted as a function of T, shown in Figs. 3(e) and 3(f), respectively. The obtained gaps can be approximated by the empirical BCS Δ–T function with $\Delta^{ab}(0) \simeq 0.50$ meV (#1) and 0.49 meV (#2). This implies a gap minimum of $\Delta^{ab}_{\min} = \Delta^{ab}(0)(1-r) \simeq 0.15$ meV. This anisotropic gap structure is highly consistent with recent ARPES observations in the momentum space of CsV_3Sb_5,[30] which is a highly anisotropic gap on the V-3d-derived β-band Fermi surface, with a gap minimum of ~ 0.10 meV.

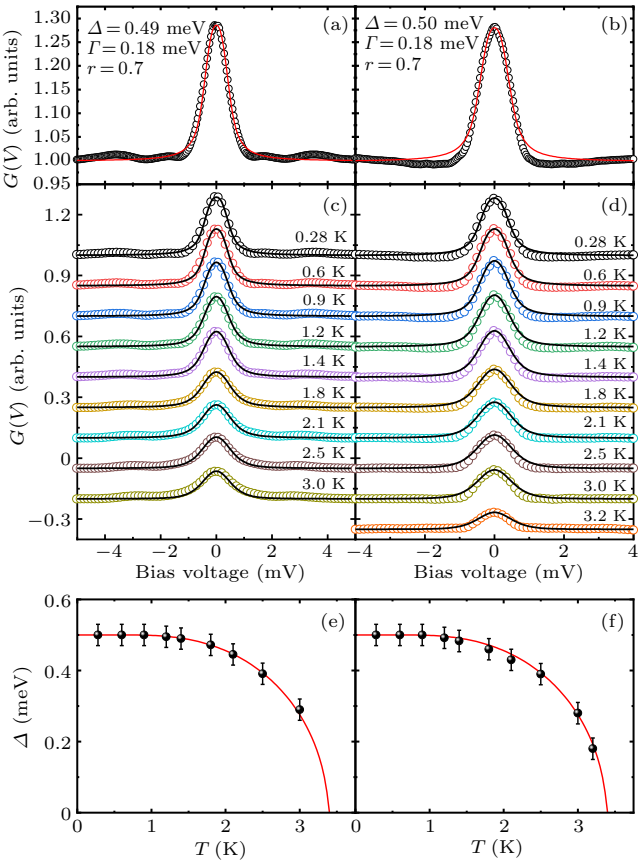


Fig. 3. (a)–(b) The normalized ab-plane Andreev conductance spectrum $G(V)/G_N$ at the lowest $T = 0.28$ K for #1 and #2 junctions, respectively. The solid red curves are their BTK fits with an anisotropic gap model. (c)–(d) The normalized ab-plane Andreev conductance spectra $G(V)/G_N$ at various T from 0.28 K to 3.5 K for #1 (c) and #2 (d) junctions, respectively. The solid curves are their BTK fits using an anisotropic gap model. All the conductance spectra and their corresponding fitting curves are shifted downward for clarity, except the top ones. (e)–(f) The corresponding superconducting gap $\Delta(T)$ as a function of T, which closely follows the BCS Δ–T function.

4. Conclusion

In summary, we performed directional soft point contact spectroscopy measurements on kagome superconductor CsV_3Sb_5 crystals. By comparison, spectral results showed that the conductance spectrum is characterized by a pronounced anisotropy in the superconducting energy gap along

the current *ab*-plane direction and full s-wave SC gaps along the *c*-axis direction. Specifically, quantitative analysis for the *ab*-plane junctions revealed an anisotropy of $\sim 70\%$ and a gap minimum of $\simeq 0.15$ meV. These results provide a foundation for further understanding the intertwinement with other electronic ordering states, such as the CDW ordering, time-reversal symmetry breaking and the topological superconducting state with Majorana flat bands on the sample edges.[47]

Acknowledgements

C.R. acknowledges financial support from the National Natural Science Foundation of China and the Joint Fund of Yunnan Provincial Science and Technology Department (Grant No. 2019FY003008). H. Wang acknowledges financial support from the National Natural Science Foundation of China (Grant No. 62164006) and Yunnan Fundamental Reseach Projects (Grant No. 202201AS07008). Y. Q. Zhao and Z. F. Wu are thankful for financial support from the "16th Graduate Research Innovation Project" of Yunnan University (Grant No. KC-24249857). H.C.L. was supported by the National Key R&D Program of China (Grant No. 2022YFA1403800) and the National Natural Science Foundation of China (Grant No. 12274459). Y.Q. was supported by the National Key R&D Program of China (Grant No. 2018YFA0704300).

References

[1] Norman M R 2016 *Rev. Mod. Phys.* **88** 041002
[2] Balents L 2010 *Nature* **464** 199
[3] Liu E K, Sun Y, Kumar N, *et al.* 2015 *Nat. Phys.* **14** 1125
[4] Liu D F, Liang A J, Liu E K, Xu Q N, Li Y W, Chen C, Pei D, Shi W J, Mo S K, Dudin P, Kim T, Cacho C, Li G, Sun Y, Yang L X, Liu Z K, Parkin S S, Felser C and Chen Y L 2019 *Science* **365** 1282
[5] Kiesel M L, Platt C and Thomale R 2013 *Phys. Rev. Lett.* **110** 126405
[6] Wang W S, Li Z Z, Xiang Y Y and Wang Q H 2013 *Phys. Rev. B* **87** 115135
[7] Ko W H, Lee P A and Wen X G 2009 *Phys. Rev. B* **79** 214502
[8] Yu S L and Li J X 2012 *Phys. Rev. B* **85** 144402
[9] Ortiz B R, Teicher S M L, Hu Y, Zuo J L, Sarte P M, Schueller E C, Abeykoon A M, Krogstad M J, Rosenkranz S, Osborn R, Seshadri R, Balents L, He J and Wilson S D 2020 *Phys. Rev. Lett.* **125** 247002
[10] Yin Q W, Tu Z J, Gong C S, Fu Y, Yan S H and Lei H C 2021 *Chin. Phys. Lett.* **38** 037403
[11] Liu Z, Zhao N, Yin Q, Gong C, Tu Z, Li M, Song W, Liu Z, Shen D, Huang Y, Liu K, Lei H and Wang S 2021 *Phys. Rev. X* **11** 041010
[12] Ortiz B R, Gomes L C, Morey J R, Winiarski M, Bordelon M, Mangum J S, Oswald I W H, Rodriguez-Rivera J A, Neilson J R, Wilson S D, Ertekin E, McQueen T M and Toberer E S 2019 *Phys. Rev. Mater.* **3** 094407
[13] Ortiz B R, Sarte P M, Kenney E M, Graf M J, Teicher S M L, Seshadri R and Wilson S D 2021 *Phys. Rev. Mater.* **5** 034801
[14] Jiang Y X, Yin J X, Denner M M, *et al.* 2021 *Nat. Mater.* **20** 1353
[15] Tan H X, Liu Y Z, Wang Z Q and Yan B H 2021 *Phys. Rev. Lett.* **127** 046401
[16] Nie L P, Sun K L, Ma W R, *et al.* 2022 *Nature* **604** 59
[17] Wilson S D and Ortiz B R 2024 *Nat. Rev. Mater.* **9** 420
[18] Jiang K, Wu T, Yin J X, Wang Z Y, Hasan M Y, Wilson S D, Chen X H and Hu J P 2023 *Nat. Sci. Rev.* **10** nwac199
[19] Song B Q, Ying T P, Wu X X, Xia W, Yin Q W, Zhang Q H, Song Y P, Yang X F, Guo J G, Gu L, Chen X L, Hu J P, Andreas S P, Lei H C, Guo Y F and Li S Y 2023 *Nat. Commun.* **14** 2492
[20] Zheng L X, Wu Z M, Yang Y, Nie L P, Shan M, Sun K Lv, Song D W, Yu F H, Li J, Zhao D, Li S J, Kang B L, Zhou Y B, Liu K, Xiang Z J, Ying J J, Wang Z Y, Wu T and Chen X H 2022 *Nature* **611** 682
[21] Asaba T, Onishi A, Kageyama Y, *et al.* 2024 *Nat. Phys.* **20** 40
[22] Mu C, Yin Q, Tu Z, Gong C, Lei H, Li Z and Luo J 2021 *Chin. Phys. Lett.* **38** 077402
[23] Duan W Y, Nie Z Y, Luo S S, Yu F H, Ortiz B R, Yin L C, Su H, Du F, Wang A, Chen Y, Lu X, Ying J J, Wilson S D, Chen X H, Song Y and Yuan H Q 2021 *Sci. China Phys. Mech. Astron.* **64** 1
[24] Yin L C, Zhang D T, Chen C F, Ye G, Yu F H, Ortiz B R, Luo S S, Duan W Y, Su H, Ying J J, Wilson S D, Chen X H, Yuan H Q, Song Y and Lu X 2021 *Phys. Rev. B* **104** 174507
[25] He M C, Zi H, Zhan H X, Zhao Y Q, Ren C, Hou X Y, Shan L, Wang Q H, Yin Q W, Tu Z, Gong C, Lei H, Lu Z Y, Wang Q, Qi Y P, Chen G F and Xiong P 2022 *Phys. Rev. B* **106** 104510
[26] Zhao C C, Wang L S, Xia W, Yin Q W, Ni J M, Huang Y Y, Tu C P, Tao Z C, Tu Z J, Gong C S, Lei H C, Guo Y F, Yang X F and Li S Y 2021 arXiv:2102.08356v2
[27] Gupta R, Das D, Mielke C H III, Guguchia Z, Shiroka T, Baines Ch, Bartkowiak M, Luetkens H, Khasanov R, Yin Q W, Tu Z J, Gong C S and Lei H C 2022 *npj Quantum Materials* **7** 49
[28] Xu H S, Yan Y J, Yin R T, Xia W, Fang S J, Chen Z Y, Li Y J, Yang W Q, Guo Y F and Feng D L 2021 *Phys. Rev. Lett.* **127** 187004
[29] Chen H, Yang H T, Hu B, Zhao Z, Yuan J, Xing Y Q, Qian G J, Huang Z H, Li G, Ye Y H, Ma S, Ni S L, Zhang H, Yin Q W, Gong C S, Tu Z J, Lei H C, Tan H X, Zhou S, Shen C M, Dong X L, Yan B H, Wang Z Q and Gao H J 2021 *Nature* **599** 222
[30] Mine A, Zhong Y, Liu J, Suzuki T, Najafzadeh S, Uchiyama T, Yin J X, Wu X, Shi X, Wang Z, Yao Y and Okazaki K 2024 arXiv.2404.18472
[31] Hu B, Chen H, Ye Y, Huang Z H, Han X H, Zhao Z, Xiao H Q, Lin X, Yang H T, Wang Z Q and Gao H J 2024 *Nat. Commun.* **15** 6109
[32] Deng H, Liu G, Guguchia Z, *et al.* 2024 *Nat. Mater.* **23** 16394
[33] Zhong Y, Liu J, Wu X, Guguchia Z, Yin J X, Mine A, Li Y, Najafzadeh S, Das D, Mielke III C, Khasanov R, Luetkens H, Suzuki T, Liu K, Han X, Kondo T, Hu J, Shin S, Wang Z, Shi X, Yao Y and Okazaki K 2023 *Nature* **617** 488
[34] Luo Y, Han Y, Liu J, Chen H, Huang Z, Huai L, Li H, Wang B, Shen J, Ding S, Li Z, Peng S, Wei Z, Miao Y, Sun X, Ou Z, Xiang Z, Hashimoto M, Lu D, Yao Y, Yang H, Chen X, Gao H J, Qiao Z, Wang Z and He J 2023 *Nat. Commun.* **14** 3819
[35] Roppongi M, Ishihara K, Tanaka Y, Ogawa K, Okada K, Liu S, Mukasa K, Mizukami Y, Uwatoko Y, Grasset R, Konczykowski M, Ortiz B R, Wilson S D, Hashimoto K and Shibauchi T 2023 *Nat. Commu.* **14** 667
[36] Wang Y, Kreisel A, Hirschfeld P J and Mishra V 2013 *Phys. Rev. B* **87** 094504
[37] Mizukami Y, Konczykowski M, Kawamoto Y, Kurata S, Kasahara S, Hashimoto K, Mishra V, Kreisel A, Wang Y, Hirschfeld P J, Matsuda Y and Shibauchi T 2014 *Nat. Commun.* **5** 5657
[38] Mizukami Y, Konczykowski M, Matsuura K, Watashige T, Kasahara S, Matsuda Y and Shibauchi T 2017 *J. Phys. Soc. Jpn.* **86** 083706
[39] Naidyuk Yu G and Yanson I K 2003 arXiv: physics/0312016
[40] Daghero D and Gonnelli R S 2010 *Supercond. Sci. Technol.* **23** 043001
[41] Mondal M, Joshi B, Kumar S, Kamlapure A, Ganguli S C, Thamizhavel A, Mandal S S, Ramakrishnan S and Raychaudhuri P 2012 *Phys. Rev. B* **86** 094520
[42] Gonnelli R S, Daghero D, Ummarino G A, Stepanov V A, Jun J, Kazakov S M and Karpinski J 2002 *Phys. Rev. Lett.* **89** 247004
[43] Deutscher G 2005 *Rev. Mod. Phys.* **77** 109
[44] Zhao C C, Wang L S, Xia W, *et al.* 2024 *Chin. Phys. Lett.* **41** 127303
[45] Iavarone M, Karapetrov G, Koshelev A E, Kwok W K, Crabtree G W, Hinks D G, Kang W N, Choi E M, Kim H J, Kim H J and Lee S I 2002 *Phys. Rev. Lett.* **89** 187002
[46] Szabó P, Samuely P, Kačmarčèk J, Klein T, Marcus J, Fruchart D, Miraglia S, Marcenat C and Jansen A G M 2001 *Phys. Rev. Lett.* **87** 137005
[47] Wang S, Feng X L, Fang J Z, *et al.* 2024 arxiv:2405.12592